Progress In Electromagnetics Research Letters, Vol. 110, 73–81, 2023

Design of a Full Polarization Reconfigurable MIMO Antenna

Jiaying Guo[1], Yiwei Ping[1], Yajuan Zhao[2], Yufeng Liu[1], and Liping Han[1, *]

Abstract—An aperture-coupled full polarization reconfigurable MIMO antenna is proposed in this letter. A cross-shaped slot loaded with PIN diodes is embedded on the ground plane, and $\pm 45^\circ$ linear polarization is realized by controlling the states of the diodes. Four slots integrated with PIN diodes are etched at the corners of the radiating patch, and then the left- and right-handed circular polarization modes are achieved by changing ON/OFF states of the diodes. Experimental results show that the antenna can achieve good impedance matching in the range of 2.4–2.46 GHz in four modes with an isolation greater than 15 dB and an axial ratio less than -3 dB in the circular polarization modes.

1. INTRODUCTION

In modern wireless systems, polarized reconfigurable technology has attracted lots of attention due to its advantages of avoiding fading loss [1]. Multiple-input multiple-output (MIMO) system can greatly increase spectrum efficiency [2]. To reduce the correlation of the system component channels, it is necessary to research polarized reconfigurable antennas in MIMO systems [3]. Usually, polarization reconfigurability is achieved using PIN diodes. In [4–7], linear polarization (LP) and circular polarization (CP) reconfigurability is realized by activating the PIN diodes embedded on the patch or ground plane. In [8], right hand circular polarization (RHCP) and left hand circular polarization (LHCP) are switched by activating the PIN diodes mounted on the feedline. In addition, RHCP and LHCP are reconfigured by exciting different ports of the antenna [9].

Full polarization reconfigurability (orthogonal linear, right-hand, and left-hand) can effectively mitigate polarization mismatch in some environments and select the best signal strength. Recently, several full polarization reconfigurable antennas have been proposed. In [10], full polarization reconfigurability is obtained by controlling the PIN diodes loaded on the metasurface. In [11], full polarization reconfigurability is achieved by changing the bias voltage of varactor diodes on a quasi-lumped coupler. In [12, 13], full polarization performance is provided by changing the bias voltage of the diodes loaded in the feeding network. In [14], quad-polarization diversity is obtained by switching the states of PIN diodes embedded in balun feeds. However, the structures of the above antennas are complicated.

In this paper, a novel full polarization reconfigurable MIMO antenna is proposed. The left- and right-hand circular polarizations and two orthogonal linear polarization modes can be obtained through controlling the states of PIN diodes. Compared with the traditional full polarized reconfigurable antenna employing a feeding network, the proposed antenna directly loads a switch on the antenna structure to control various polarization modes, which makes the antenna structure simpler.

Received 20 March 2023, Accepted 29 April 2023, Scheduled 8 May 2023

* Corresponding author: Liping Han (hlp@sxu.edu.cn).

[1] School of Physics and Electronic Engineering, Shanxi University, Taiyuan 030006, China. [2] No. 33 Research Institute of China Electronics Technology Group Corporation, Taiyuan 030006, China.

2. ANTENNA DESIGN AND PRINCIPLE

2.1. Antenna Design

The geometry of the aperture-coupled full polarization reconfigurable MIMO antenna is shown in Fig. 1. The antenna elements are placed in parallel. Two radiating patches are printed on the top of substrate 1. The ground plane and feed line are printed on the top and bottom sides of substrate 2, respectively. As shown in Figs. 1(b) and (c), four slots embedded with PIN diodes S_1–S_4 are etched at four corners of the patch, and a cross-shaped slot integrated with PIN diodes S_5–S_8 is etched at the center of the ground plane. The diodes used in the design are BAR50-02V, which are equivalent to a resistor of 3 Ω for ON state and a resistor of 5 kΩ in parallel with a capacitor of 0.15 pF for OFF state.

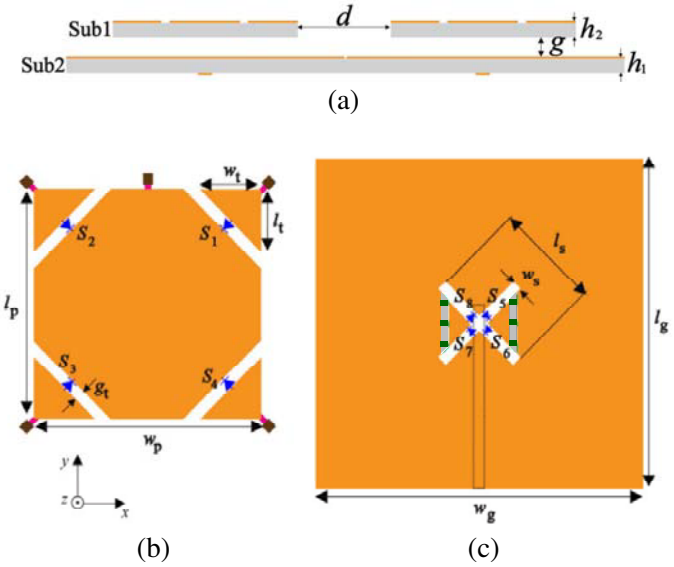

Figure 1. Configuration of antenna. (a) Side view of MIMO antenna, (b) patch of antenna element, (c) ground of antenna element, (green-capacitors, pink-inductors, brown-biasing pads).

In order to provide bias for S_1–S_4, five pads are printed along the edges of the patch, and five inductors of 12 nH are loaded to block the RF signal patches. Two narrow slits (marked as gray) are introduced on the ground plane to provide bias for S_5–S_8, and six dc block capacitors of 100 pF are loaded on the narrow slits to avoid dc signal flowing into the RF source and provide RF wave connection throughout the ground plane. The triangular area enclosed by the cross-shaped slot and narrow slits serves as a DC electrode of diode, while another DC electrode is provided by the metal outside the triangular area. The left- and right-handed circular polarization modes can be obtained through controlling the ON/OFF states of S_1–S_4, and two orthogonal linear polarization modes can be achieved by changing the states of S_5–S_8. The chosen substrates are FR4 with a relative permittivity of 4.4, and the software used in the simulation process is HFSS. The optimized parameters are: $h_1 = 1.6$ mm, $h_2 = 0.8$ mm, $g = 4$ mm, $l_p = w_p = 44$ mm, $l_t = 12$ mm, $w_t = 12$ mm, $g_t = 1$ mm, $l_g = w_g = 75$ mm, $l = 50$ mm, $w_s = 2$ mm, $l_s = 20$ mm, $p_s = 37.5$ mm, $d = 25$ mm.

Table 1 lists the operating modes of the antenna. In order to realize the circular polarization operation, diodes S_5–S_8 are turned off. In mode 1 (S_1 and S_3 on, S_2 and S_4 off), the chamfers in the $-45°$ direction perturb the surface current path in the patch, and the left-hand circular polarization is generated. Similarly, in mode 2 (S_1 and S_3 off, S_2 and S_4 on), the chamfers in the $+45°$ direction act as the perturbing elements, and the right-hand circular polarization is achieved. It is well known that, for a linear polarization antenna, the antenna performance is not affected by the chamfers on the patch. To cover the required working frequency band in the linear polarization modes, the upper (S_1 and S_2) and lower diodes (S_3 and S_4) are turned off and on, respectively. In mode 3 (S_5 and S_7 on, S_6 and S_8 off), the power radiated from the feedline is coupled to the patch through the slot in the $-45°$ direction,

Table 1. Operate modes of antenna.

	S_1	S_2	S_3	S_4	S_5	S_6	S_7	S_8
Mode 1	On	Off	On	Off	Off	Off	Off	Off
Mode 2	Off	On	Off	On	Off	Off	Off	Off
Mode 3	Off	Off	On	On	On	Off	On	Off
Mode 4	Off	Off	On	On	Off	On	Off	On

so $+45°$ linear polarization is realized. In the same way, the electromagnetic energy is coupled to the patch by the slot in the $+45°$ direction, and $-45°$ linear polarization is obtained.

2.2. Working Principle

To illustrate the working mechanism of the proposed MIMO antenna, the surface current distribution is investigated, as shown in Fig. 2. The current distribution characteristics of each mode can be clearly seen from this figure. From Fig. 2(a), it is observed that, in mode 1, the current of two antenna elements rotates clockwise in one period, and that the antenna can achieve LHCP. Similarly, the antenna achieves RHCP in mode 2 due to the current rotating counterclockwise in one period, as shown in Fig. 2(b). In modes 3 and 4, as illustrated in Figs. 2(c) and (d), the surface current flows in the $+45°$ direction and $-45°$ direction, and the antenna achieves $+45°$ and $-45°$ linear polarizations.

The effect of the structural parameters on the antenna performance is also conducted. It is found that the circular polarization modes are mainly influenced by the length of corner patches (l_t), and the linear polarization modes are affected by the coupling slot (l_s). Figs. 3 and 4 show the S-parameter and axial ratio (AR) for different l_t in modes 1 and 2, respectively. From Figs. 3 and 4, it is observed that the impedance bandwidth and axial ratio bandwidth of CP are sensitive to l_t. With the increase of l_t, the antenna impedance bandwidth increases, and the axial ratio of LHCP shifts toward lower frequency. Fig. 5 shows the S-parameter for different l_s in modes 3 and 4. It is observed that the resonant frequency shifts toward lower frequency, and the impedance bandwidth increases with the increase of l_s. When $l_t = 12\,\text{mm}$ and $l_s = 20\,\text{mm}$, the S_{11} covers the working frequency band in four modes, and 3 dB axial ratio bandwidth covers 2.4–2.46 GHz.

3. RESULTS AND DISCUSSION

To confirm the property of the full polarization reconfigurable MIMO antenna, a prototype was fabricated and measured, as shown in Fig. 6. The simulated and measured S-parameters are given in Fig. 7. The measured results are in good agreement with the simulated ones. The measured $-10\,\text{dB}$ impedance bandwidths in four modes are: 2.16–2.84 GHz, 2.16–2.79 GHz, 2.36–2.48 GHz, and 2.37–2.49 GHz. The S_{21} is less than $-15\,\text{dB}$ in all four modes, which indicate that a good port isolation performance is obtained. The measured bandwidth is a little wider than the simulated one, which may be caused by the tolerance existing in the antenna prototype fabrication.

The AR of antenna in circularly polarization modes is shown in Fig. 8. The $-3\,\text{dB}$ AR bandwidths for modes 3 and 4 are 66 MHz and 59 MHz, respectively. Considering the S-parameters of antenna, full polarization performance can be achieved in the range of 2.4 GHz–2.46 GHz with an overlapped bandwidth of 2.7%.

Figure 9 shows the normalized measured radiation pattern of antenna at 2.43 GHz. It can be seen that a broadside radiation pattern can be obtained for all four modes. The half-power bandwidth (HPBW) in circular polarization modes is 83°, while for the linear polarization modes, the HPBWs are 77° and 110° in E-plane and H-plane. The realized gain of antenna is given in Table 2. The gains of the ports in circularly polarization and linear polarization modes are greater than 5.71 dBi and 5.6 dBi, respectively.

Envelope correlation coefficient (ECC) is an important parameter to evaluate the diversity performance of MIMO antennas. ECC can be calculated through S-parameters [15] and far-field

Table 2. Realized gain in different modes of antenna.

		Mode 1	Mode 2	Mode 3	Mode 4
Realized gain (dBi)	Port 1	5.78	5.82	5.6	5.64
	Port 2	5.71	5.84	5.68	5.63

radiation patterns [16] using Equations (1) and (2), respectively. The ECC of the antenna is shown in Fig. 10. It can be seen that the ECC based on S-parameters is lower than 0.05, and that based on radiation patterns is lower than 0.5 in the range of 2.16–2.84 GHz. Therefore, the proposed antenna has

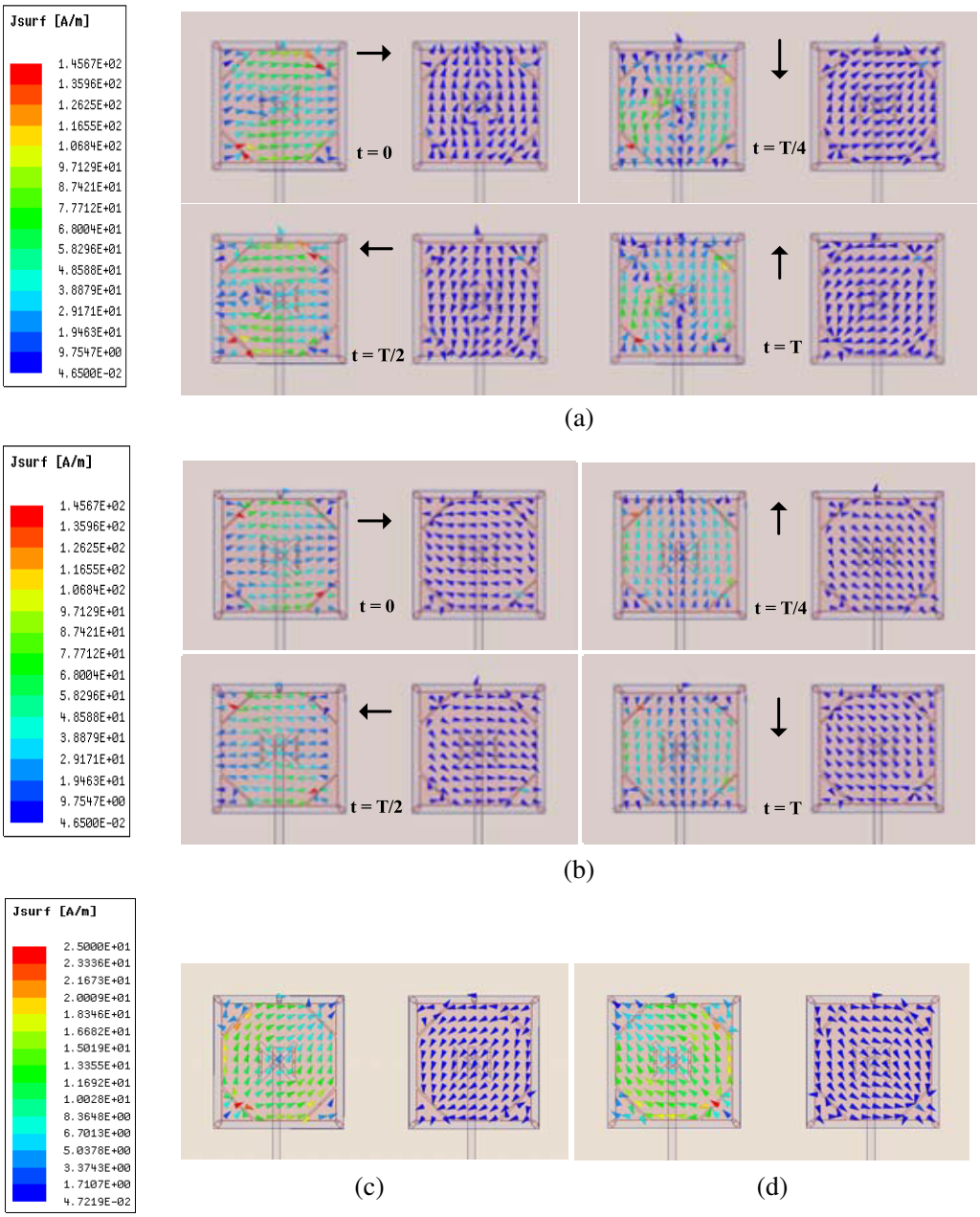

Figure 2. Simulated current distributions of antenna in (a) mode 1, (b) mode 2, (c) mode 3, (d) mode 4.

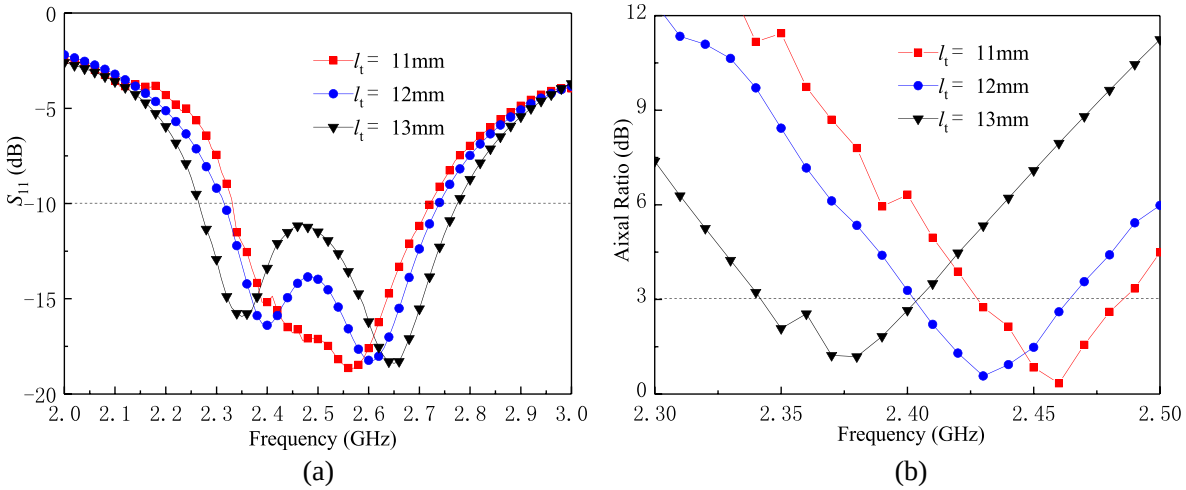

Figure 3. S-parameter and AR for different l_t in mode 1. (a) S-parameter, (b) AR.

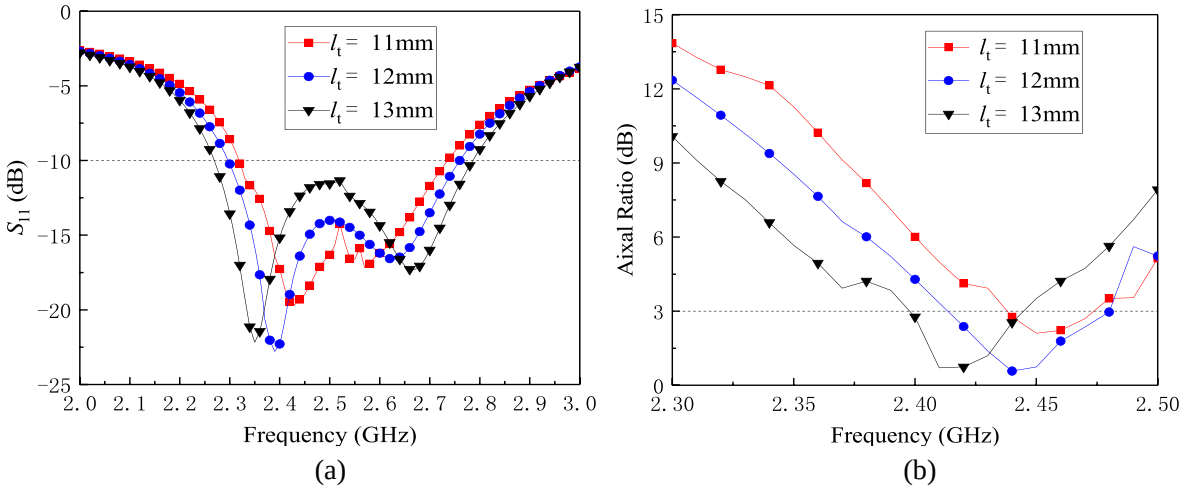

Figure 4. S-parameter and AR for different l_t in mode 2. (a) S-parameter, (b) AR.

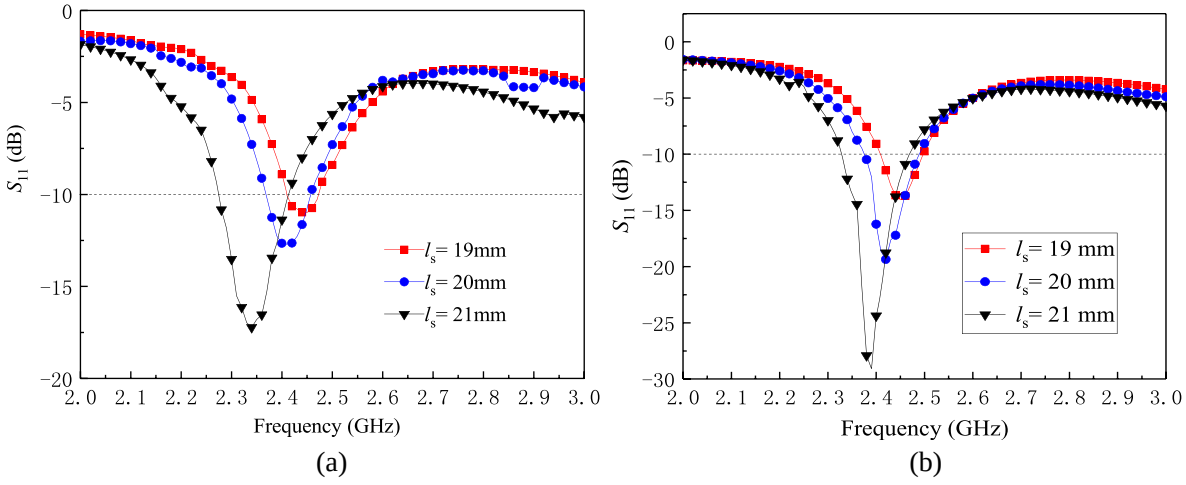

Figure 5. S-parameter for different l_s in (a) mode 3, (b) mode 4.

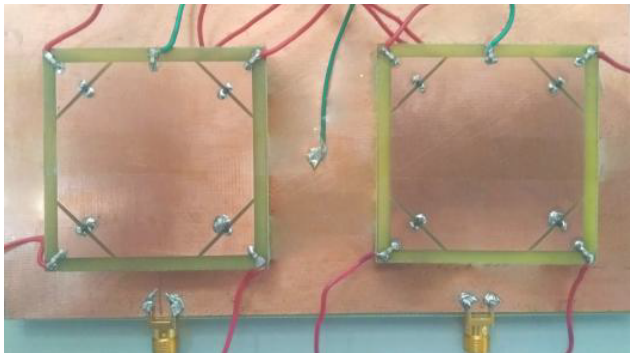

Figure 6. Photograph of fabricated antenna.

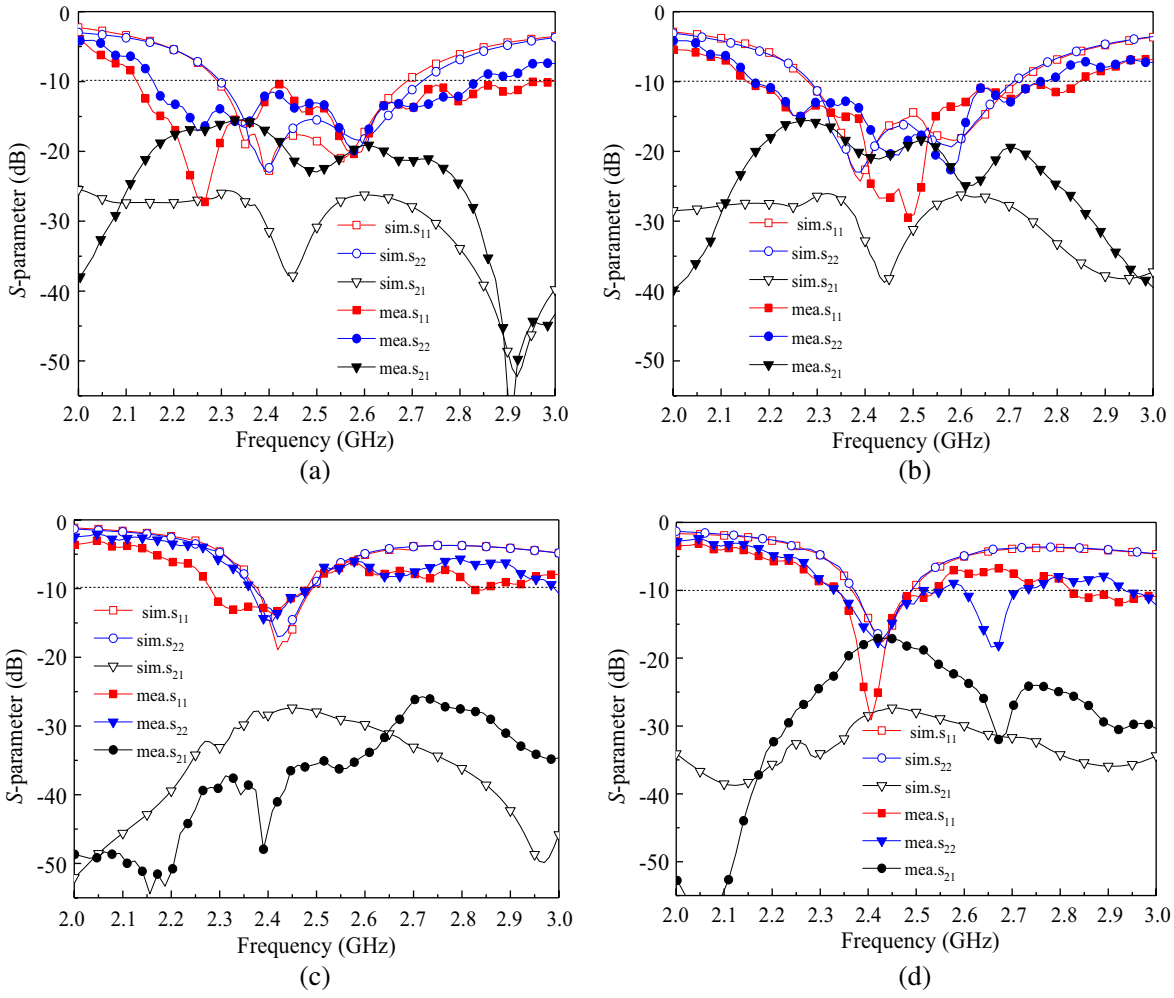

Figure 7. *S*-parameter results of antenna in (a) mode 1, (b) mode 2, (c) mode 3, (d) mode 4.

good diversity capability.

$$\rho_e = \frac{\left|S_{11}^* S_{12} + S_{21}^* S_{22}\right|^2}{\left(1 - |S_{11}|^2 - |S_{21}|^2\right)\left(1 - |S_{22}|^2 - |S_{12}|^2\right)} \tag{1}$$

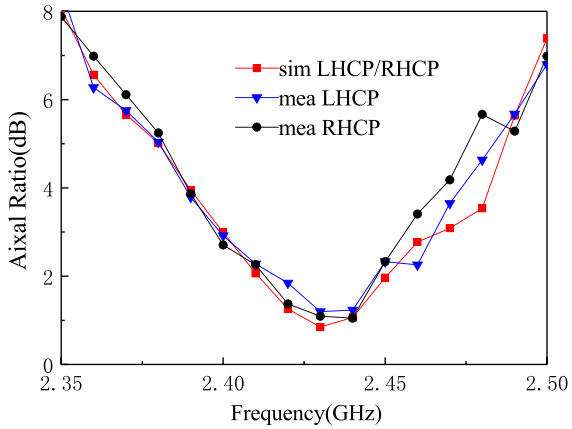

Figure 8. AR of antenna.

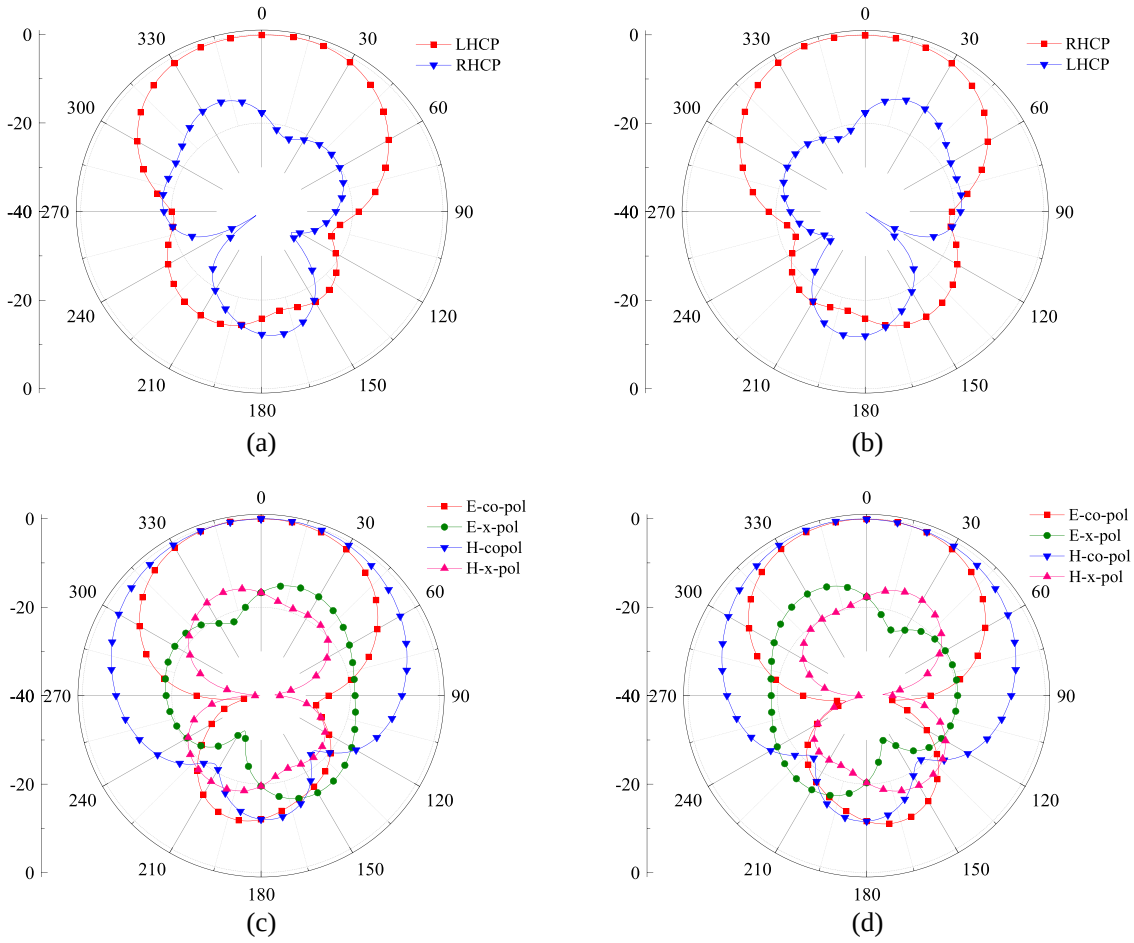

Figure 9. Radiation pattern of antenna in (a) mode 1, (b) mode 2, (c) mode 3, (d) mode 4.

$$\rho_e = \frac{\left|\iint_{4\pi} \left[F_{porti}\left(\theta,\varphi\right) * F_{portj}\left(\theta,\varphi\right)\right] d\Omega\right|^2}{\iint_{4\pi} \left|F_{porti}\left(\theta,\varphi\right)\right|^2 d\Omega \iint_{4\pi} \left|F_{portj}\left(\theta,\varphi\right)\right|^2 d\Omega} \tag{2}$$

Finally, Table 3 lists the comparison of the reported and proposed full polarization reconfigurable

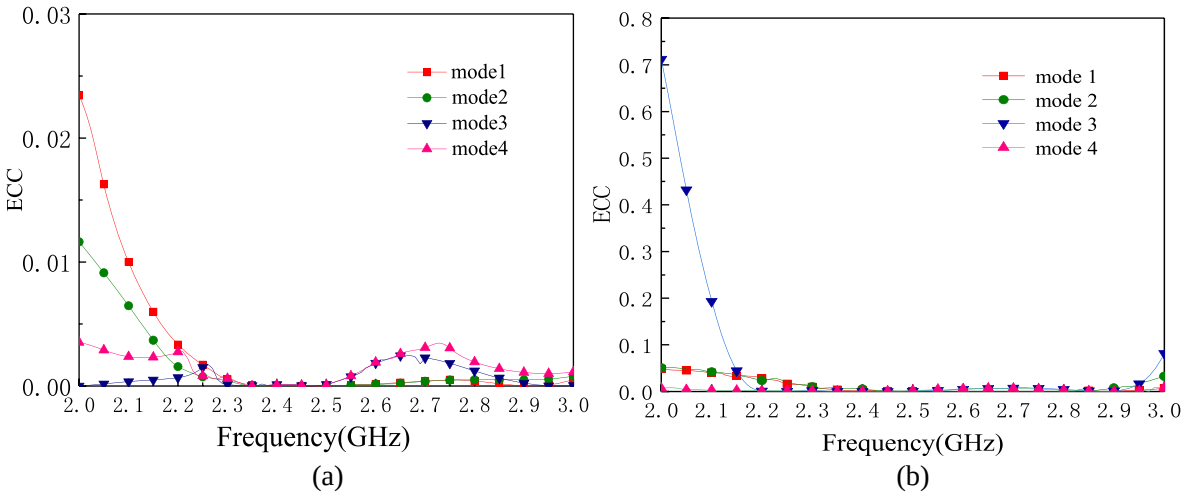

Figure 10. ECC of antenna through. (a) S-parameters. (b) Radiation patterns.

Table 3. Performance comparison of full polarization reconfigurable antennas.

Refs.	Antenna size (λ_0^3)	Frequency (GHz)	IBW (%)	ARBW (%)	Peak gain (dBi)
[10]	$1.30 \times 1.30 \times 0.067$	4–5.25	25 (CP), 21.7 (LP)	1	5.49
[11]	$0.32 \times 0.25 \times 0.010$	3.3–3.6	2.8 (CP), 1.4 (LP)	3.7	6.2
[12]	$0.35 \times 0.35 \times 0.021$	2.4–2.5	4 (CP), 3.6 (LP)	-	5
[13]	$8.00 \times 5.00 \times 0.100$	28–32	13.3 (CP), 13.3 (LP)	13.3	11.3
[14]	$0.90 \times 0.90 \times 0.170$	1.5–2.3	42.1 (CP), 35.8 (LP)	42.1	7
This work	$0.63 \times 0.63 \times 0.053$	2.16–2.84	27.2 (CP), 4.9 (LP)	4.2	5.82

antennas. It can be seen that the proposed antenna has larger CP bandwidth than the antennas with similar gains [10–12]. Moreover, the antenna in this work has smaller size than the antennas in [13, 14].

4. CONCLUSIONS

A full polarization reconfigurable MIMO antenna that can operate in four modes: left-handed circular polarization, right-handed circular polarization, and $\pm 45°$ linear polarization is presented. Circular polarization and linear polarization can be controlled by the PIN diodes embedded in the patch and ground, respectively. The overlapped bandwidth of antenna in four modes is 2.7%, and the isolation is greater than 15 dB. The ECC is close to zero in the overlapped band. Compared with the traditional full polarized reconfigurable antenna employing the feeding network, the proposed antenna directly loads the switch on the antenna structure to control various polarization modes, which makes the antenna structure simpler.

ACKNOWLEDGMENT

This work is supported by the National Natural Science Foundation of China (62071282), and in part by the Natural Science Foundation of Shanxi Province (201901D111026).

REFERENCES

1. Park, J., M. Choo, S. Jung, D. Choi, J. Choi, and W. Hong, "A software-programmable directivity, beamsteering, and polarization reconfigurable block cell antenna concept for millimeter-wave 5G phased-array architectures," *IEEE Transactions on Antennas and Propagation*, Vol. 69, No. 1, 146–154, 2021.
2. Kumar, A., G. Saxena, P. Kumar, et al., "Quad-band circularly polarized super-wideband MIMO antenna for wireless applications," *International Journal of RF and Microwave Computer-Aided Engineering*, Vol. 32, No. 6, e23129, 2022.
3. Bhattacharjee, A. and S. Dwari, "A monopole antenna with reconfigurable circular polarization and pattern tilting ability in two switchable wide frequency bands," *IEEE Antennas and Wireless Propagation Letters*, Vol. 20, No. 9, 1661–1665, 2021.
4. Yoon, W. S., J. W. Baik, H. S. Lee, S. Pyo, S. M. Han, and Y. S. Kim, "A reconfigurable circularly polarized microstrip antenna with a slotted ground plane," *IEEE Antennas and Wireless Propagation Letters*, Vol. 9, 1161–1164, 2010.
5. Qin, P. Y., A. R. Weily, Y. J. Guo, and C. H. Liang, "Polarization reconfigurable U-slot patch antenna," *IEEE Transactions on Antennas and Propagation*, Vol. 58, No. 10, 3383–3388, 2010.
6. Begum, H., X. Wang, and M. Lu, "A polarization-reconfigurable microstrip antenna design based on parasitic pin loading," *IEEE Radio and Wireless Symposium (RWS)*, 135–137, 2017.
7. Chen, Q., J.-Y. Li, G. Yang, B. Cao, and Z. Zhang, "A polarization-reconfigurable high-gain microstrip antenna," *IEEE Transactions on Antennas and Propagation*, Vol. 67, No. 5, 3461–3466, 2019.
8. Lin, W. and H. Wong, "Wideband circular-polarization reconfigurable antenna with L-shaped feeding probes," *IEEE Antennas and Wireless Propagation Letters*, Vol. 16, 2114–2117, 2017.
9. Kumar, A., A. Q. Ansari, B. K. Kanaujia, et al., "Dual circular polarization with reduced mutual coupling among two orthogonally placed CPW-fed microstrip antennas for broadband applications," *Wireless Personal Communications*, No. 107, 759–770, 2019.
10. Li, W., Y. M. Wang, Y. Hei, B. Li, and X. Shi, "A compact low-profile reconfigurable metasurface antenna with plarization and pattern diversities," *IEEE Antennas and Wireless Propagation Letters*, Vol. 20, No. 7, 1170–1174, 2021.
11. Ferrero, F., C. Luxey, R. Staraj, G. Jacquemod, M. Yedlin, and V. Fusco, "A novel quad-polarization agile patch antenna," *IEEE Transactions on Antennas and Propagation*, Vol. 57, No. 5, 1563–1567, 2009.
12. Wu, Y. F., C. H. Wu, D. Y. Lai, and F. C. Chen, "A reconfigurable quadri-polarization diversity aperture-coupled patch antenna," *IEEE Transactions on Antennas and Propagation*, Vol. 55, No. 3, 1009–1012, 2007.
13. Sun, Q., Y. L. Ban, Y. Liu, and F. Q. Yan, "Millimeter-wave switchable quadri-polarization array antenna based on folded C-type SIW," *IEEE Antennas and Wireless Propagation Letters*, Vol. 20, No. 6, 1088–1092, 2021.
14. Row, J. S. and Y. H. Wei, "Wideband reconfigurable crossed-dipole antenna with quad-polarization diversity," *IEEE Transactions on Antennas and Propagation*, Vol. 66, No. 4, 2090–2094, 2018.
15. Kang, L., H. Li, X. Wang, and X. Shi, "Compact offset microstrip-fed MIMO antenna for band-notched UWB applications," *IEEE Antennas and Wireless Propagation Letters*, Vol. 14, 1754–1757, 2015.
16. Kumar, A., A. Q. Ansari, B. K. Kanaujia, J. Kishor, and L. Matekovits, "A review on different techniques of mutual coupling reduction between elements of any MIMO antenna. Part 1: DGSs and parasitic structures," *Radio Science*, Vol. 56, No. 3, 1–25, 2021.